TISSUE ENGINEERING: Part A
Volume 15, Number 4, 2009

DOI: 10.1089/ten.tea.2008.0223

Optical Mapping of Impulse Propagation in Engineered Cardiac Tissue

Milica Radisic, Ph.D.,[1] Vladimir G. Fast, Ph.D.,[2] Oleg F. Sharifov, Ph.D.,[2] Rohin K. Iyer, B.A.Sc.,[1] Hyoungshin Park, Ph.D.,[3,4] and Gordana Vunjak-Novakovic, Ph.D.[5]

Cardiac tissue engineering has a potential to provide functional, synchronously contractile tissue constructs for heart repair, and for studies of development and disease using *in vivo*–like yet controllable *in vitro* settings. In both cases, the utilization of bioreactors capable of providing biomimetic culture environments is instrumental for supporting cell differentiation and functional assembly. In the present study, neonatal rat heart cells were cultured on highly porous collagen scaffolds in bioreactors with electrical field stimulation. A hallmark of excitable tissues such as myocardium is the ability to propagate electrical impulses. We utilized the method of optical mapping to measure the electrical impulse propagation. The average conduction velocity recorded for the stimulated constructs (14.4 ± 4.1 cm/s) was significantly higher than that of the nonstimulated constructs (8.6 ± 2.3 cm/s, $p = 0.003$). The measured electrical propagation properties correlated to the contractile behavior and the compositions of tissue constructs. Electrical stimulation during culture significantly improved amplitude of contractions, tissue morphology, and connexin-43 expression compared to the nonsimulated controls. These data provide evidence that electrical stimulation during bioreactor cultivation can improve electrical signal propagation in engineered cardiac constructs.

Introduction

Cardiac tissue engineering has a potential to provide functional tissue constructs for repair of myocardial infarction and congestive heart failure that currently affect close to 12 million people in the United States alone.[1] In an envisioned scenario, the scar tissue resulting from pathological remodeling after myocardial infarction can be replaced by a synchronously contracting engineered cardiac patch. In contrast to skeletal tissues such as bone or cartilage where patients can be asked to reduce the load bearing function of these tissues for a period of time, some degree of functionality of an engineered cardiac patch is required immediately, at the time of implantation. Importantly, engineered tissues that are being developed for applications in regenerative medicine can also find utility on a much shorter time scale in studies of development, disease progression, and drug screening, and in many other applications in biological and medical research.

One paradigm of tissue engineering is that the reparative cells can be induced to form functional tissue constructs *in vitro* by cultivation on biomaterial scaffolds in bioreactors, with these two components jointly providing the necessary cues for cell differentiation and tissue assembly. A large number of scaffolds that are biodegradable and biocompatible are available for cardiac tissue engineering,[2–8] and significant efforts in the field of stem cell biology are underway to find clinically relevant source of cardiomyocytes.[9–11] Most recently, an exciting possibility of induced pluripotency (iPS) cells emerged, and it may be envisioned that iPS cells will provide an autologous source of millions of cardiomyocytes required for tissue engineering of human cardiac patches.[12–16]

However, it is the cultivation in bioreactors that enables us to engineer contractile cardiac tissues *in vitro* and modulate their functional properties. Our work is focused on developing bioreactor systems for cardiac tissue engineering using neonatal rat cardiomyocytes as a model cell source, while we anticipate that the same bioreactor systems will be translated to clinically relevant sources of human cardiomyocytes.

We reported previously that cultivation of engineered cardiac tissue in the presence of electrical field stimulation (square pulses at the frequency of 1 Hz, signal amplitude of 5 V/cm, and signal duration of 2 ms) remarkably improved cardiomyocyte function in engineered myocardium.[17] The surface of the stimulated tissue consisted of elongated cells expressing cardiac differentiation markers, sarcomeric α-actin,

[1]Institute of Biomaterials and Biomedical Engineering, University of Toronto, Toronto, Ontario, Canada.
[2]Department of Biomedical Engineering, University of Alabama at Birmingham, Birmingham, Alabama.
[3]Department of Surgery, Massachusetts General Hospital, Harvard Medical School, Boston, Massachusetts.
[4]Department of Chemical Engineering, Massachusetts Institute of Technology, Cambridge, Massachusetts.
[5]Department of Biomedical Engineering, Columbia University Vanderbilt Clinic, New York, New York.

cardiac troponin I, and α and β myosin heavy chain. Remarkably well-developed sarcomeres and gap junctions could be seen by transmission electron microscopy.[17]

In native myocardium, cardiomyocytes form a three-dimensional syncytium that enables propagation of electrical signals across gap junctions to produce coordinated mechanical contractions that pump blood forward. Groups of specialized cardiac myocytes (pace makers) generate electrical impulses that are propagated through the ventricles to drive periodic contractions of the heart. Excitation of each cardiac myocyte is followed by the increase in the amount of cytoplasmic calcium that in turn triggers mechanical contraction. Electrical propagation is therefore critical for the function of the heart. Engineered constructs that cannot propagate electrical signals would have no utility for implantation because they may result in conduction blocks or generation of arrhythmia when implanted in the ventricles. Thus, engineered cardiac tissues need to be evaluated for impulse propagation.[18] In the present study, we focused on the characterization of electrical impulse propagation by using optical mapping, and the method was used to determine the effects of electrical stimulation during cultivation on functional properties in the resulting tissue constructs.

Our second objective was to investigate the effects of the presence of nonmyocytes on engineered myocardium, as our previous study focused exclusively on the identification and characterization of cardiomyocytes.[17] Cardiomyocytes account for only one third of all the cells found in the native myocardium. However, due to their large size they occupy 90% of the volume and are critically responsible for contractile function.[19,20] The remaining two thirds of the cells are fibroblasts and endothelial cells, with smaller numbers of pericytes, smooth muscle cells, and macrophages.[19,20] Fibroblasts secrete components of the extracellular matrix and soluble factors, and transduce mechanical signals.[20,21] Endothelial cells line the dense coronary vasculature and regulate the autocrine and paracrine signaling important in angiogenesis.[22] Both cell types interact with cardiomyocytes to coordinate tissue structure and function, and the presence of both myocytes and nonmyocytes in the engineered 3D cardiac tissue may be required for appropriate function.[23,24]

Materials and Methods

Neonatal rat heart cells

Neonatal (1–2 days old) Sprague-Dawley rats were euthanized according to the procedure approved by the Institute's Committee on Animal Care. The hearts were removed and quartered, and the cells were isolated by an overnight treatment with trypsin (4°C, 6120 units/mL in Hank's balanced salt solution, HBSS) followed by serial collagenase digestion (220 units/mL in HBSS) as described in previous work.[25] The supernatants from five collagenase digests of the tissues were collected and centrifuged at 750 rpm (94 *g*) for 4 min, resuspended in culture medium, and preplated into T75 flasks (BD Biosciences, Bedford, MA) for one 1 h interval to enrich the cell suspension for cardiomyocytes. The culture medium consisted of Dulbecco's modified Eagle's medium (Gibco, Billings, MT) with 4.5 g/L glucose, 4 mM L-glutamine, 10% certified fetal bovine serum (Gibco), 100 U/mL penicillin, 100 μg/mL streptomycin, and 10 mM 4-2-hydroxyethyl-1-piperazineethanesulfonic acid buffer (HEPES; Gibco).

Collagen scaffold

The scaffolds were commercially available collagen sponges, Ultrafoam™ (Davol). Dry collagen scaffold was cross-sectioned using a sharp razor blade, sputter coated with gold, and imaged in face and cross section using Hitachi S3400N Variable Pressure Scanning Electron Microscope at the Microscopy Imaging Laboratory, University of Toronto. For imaging of the scaffold in the hydrated state, the scaffolds were wetted in phosphate buffer saline and placed on the scanning electron microscope stage with temperature set to 0°C, and the pressure was adjusted during imaging as required to prevent formation of ice crystals and to obtain clear images.

Construct preparation

Ultrafoam collagen sponge scaffolds (8×14×1.5 mm) were prewetted with culture medium and placed into the 37°C/5% CO_2 humidified incubator (Napco, Winchester, VA) for 1 hour before inoculation. Cells (14×10^6) were pelleted by centrifugation (1000 rpm, 10 min) and resuspended in Matrigel® (70 μL, Becton-Dickinson) while working on ice to prevent premature gelation as we described previously.[2] Prewetted scaffolds were gently blotted dry and placed in six-well plates (one/well), and the Matrigel/cell suspension was delivered evenly to the top surface of each scaffold using an automatic pipette. Gelation was achieved within 15 min at 37°C. Subsequently, culture medium was added (4 mL/well), and the plates were orbitally mixed (25 rpm) for 3 days. For reverse-transcription and polymerase chain reaction (RT-PCR), the constructs were prepared and stimulated in an identical manner except that the thinner sponges (8×6×0.25 mm) were seeded with 1 million cells; thus, the initial cell seeding density was identical.

Electrical stimulation

After 3 days of cultivation without electrical stimulation, the constructs were transferred to a chamber consisting of a 100 mm glass Petri dish fitted with two 1/8-inch-diameter carbon rods (Ladd Research Industries, Williston, VT) placed at a distance of 1 cm and connected to a commercial cardiac stimulator (Nihon Kohden, Tokyo, Japan) via platinum wires (Ladd Research Industries).[25] Silicone tubing (Cole-Parmer, Vernon Hills, IL) spacers were used to create six wells between the two electrodes, enabling the cultivation of six constructs per dish (Fig. 1A). In one group (designated "stimulated"), the constructs were stimulated with square pulses, 2 ms in duration, supra-threshold amplitude of 5 V (field strength of 5 V/cm), frequency of 1 Hz for the remainder of cultivation (8 days). This stimulation voltage was selected to induce synchronous construct contractions (observable with optical microscope at 10× magnification). Construct placed in an identical chamber but without electrical stimulation served as control (designated "non-stimulated"). All chambers were orbitally mixed at 25 rpm. Experiments were performed in a 37°C/5% CO_2 humidified incubator. The evaluation of construct's functional properties and immunohistochemistry were performed at the end of cultivation (8 days) as described below.

The excitation threshold of engineered cardiac constructs was evaluated at the end of cultivation before optical mapping studies, by monitoring contractile activity upon electrical stimulation at 10× magnification using a microscope (Nikon Diaphot, Melville, NY).[17] Each construct that was evaluated was placed in a 100 mm Petri dish containing

120 mL of Tyrode's solution (140 mM NaCl, 5.4 mM KCl, 0.33 mM NaH_2PO_4, 1.8 mM $CaCl_2$, 1 mM MgCl2, 5 mM HEPES, 5.5 mM D-glucose, pH 7.4) between two custom-made gold electrodes connected to a cardiac stimulator (Nihon Kohden). The temperature was maintained at 29°C using a heating tape (VWR International, Bridgeport, NJ) attached to the bottom of the Petri dish. The stimuli (square pulses, 2 ms duration) were applied at a rate of 1 Hz starting at the amplitude of 1 V. The amplitude was increased in 0.1 V increments until the entire construct was observed to beat synchronously, a voltage defined as the excitation threshold. To measure the amplitude of contractions, video-recorded beating sequences (1–5 min in duration) were digitized at the rate of 30 frames/s. The en-face area of each construct was measured as function of time using image analysis (Scion Image software, Scion, Frederick, MD). Plots of the construct en-face area versus time were constructed and used to determine the base-line area of the construct in the relaxed state. Deviation of the construct area greater than ~0.5% from this baseline was considered to be the start of a contraction. The time at which the construct area returned to the base-line value was considered to be the end of a contraction. Duration of contraction was determined as the time period between the start and end of the contraction. Amplitude of contraction was expressed as fractional area change.

Optical mapping

For optical measurements, tissue constructs were transferred into a perfusion bath and superfused with Hanks balanced salt solution having a composition of (mM): NaCl 137, KCl 5.4, KH_2PO_4 0.4, NaH_2PO_4 0.4, $MgSO_4$ 0.8, $CaCl_2$ 1.3, $NaHCO_3$ 4.2, HEPES 5.0, and glucose 5.1. The pH of the solution was 7.4, and the temperature was kept constant at 35°C. Tissue constructs were stained with 5 μM solution of fluorescent Vm-sensitive dye RH-237 (Molecular Probes, Eugene, OR). Dye fluorescence was excited using a 200-W Hg/Xe lamp at 530–585 nm, and emitted fluorescence was measured at >650 nm using a microscopic mapping system described previously.[26,27] The system included a 16×16 photodiode array (Hamamatsu Corporation, Bridgewater, NJ) and an inverted microscope (Axiovert 135TV; Zeiss, Jena, Germany) with 5× and 10× objective lenses (Fluar, Zeiss, Jena, Germany) allowing optical recordings at spatial resolutions of 110 and 55 μm/diode. Tissue constructs were paced at 400-ms cycle length using a bipolar electrode. Local activation times were measured at the 50% level of action potential upstrokes. Activation maps were constructed using linear interpolation and triangulation algorithms between neighboring recording locations. At each location, conduction velocity was calculated using activation times at four neighboring sites. Conduction velocity values from all sites were used to calculate the average map conduction velocity.

Histology and immunostaining

At the end of cultivation the constructs were fixed in formalin for 24 h and paraffin embedded. The constructs were sections such that the face-sectional area within the first 200 μm of the construct surface was revealed. The 5-μm paraffin sections were deparaffinized and stained with hematoxylin and eosin, Mason's trichrome, and smooth muscle actin, at the Toronto General Hospital Pathology and Histology Laboratory, using standard protocols. Sections were also immunostained in-house, with antibodies to monoclonal rabbit anti-cardiac troponin I (DF 1:150; Chemicon, Temecula, CA), monoclonal rat anti-vimentin (Cy3 conjugated, DF 1:50; Sigma, St. Louis, MO), and polyclonal rabbit anti-von Willebrand factor (DF 1:150; Chemicon) as we described previously.[28,29] Cell nuclei counterstaining with 4′,6-diamidino-2-phenylindole (DAPI) was done in the mounting step using mounting medium containing DAPI (Vector Laboratories, Burlingame, CA). Normal horse serum (10% in phosphate buffered saline; Vector Laboratories) was used for blocking prior to staining. Primary staining was done overnight at 4°C in a humidified chamber. Slides were incubated with secondary antibody for 30 min at room temperature in a humidified chamber using fluorescein isothiocyanate goat anti-mouse (DF 1:64; Sigma) or fluorescein isothiocyanate goat anti-rabbit (DF 1:200; Vector Laboratories) as required. Optical microscopy images were taken using a Canon PC1145 Powershot A620 Camera. Fluorescence imaging was performed on a Leica DMIRE2 microscope, and images were captured using Openlab 4.0.4 software.

RNA extraction

At the end of cultivation the constructs ($n = 3$ nonstimulated, 3 stimulated) were transferred into 1.5 mL RNAse- and DNAse-free tubes. The constructs were snap frozen by placing the tubes directly into liquid nitrogen and immersing them for 2 h. The constructs were then thawed at room temperature for 10 min before addition of 0.5 mL of TRIzol reagent (Invitrogen, Carlsbad, CA) to each tube for total RNA extraction.

The samples were incubated in TRIzol at room temperature for 20 min, with occasional pipetting to facilitate cell dissociation. 100 μL of chloroform was added to each tube, followed by brief vortexing and centrifuging at 11000 rpm (7440 *g*) for 15 min to separate the aqueous and organic phases. The aqueous (RNA-containing) phase was then transferred to a new tube, and the RNA was precipitated by addition of 250 μL of 2-propanol to each tube followed by incubation at −80°C for 1 h. RNA was pelleted by centrifuging at 11,000 rpm (7440 *g*) for 10 min and then washed by adding 500 μL of 75% ethanol and briefly vortexing each tube. The RNA was again pelleted at 8800 rpm (4762 *g*) for 5 min, and the supernatant discarded. The pellet, containing total RNA, was then dissolved in 50 L of DNAse- and RNAse-free distilled water and quantified using an absorption, single-beam biophotometer (Eppendorf, Hamburg, Germany).

Reverse-transcription and polymerase chain reaction

Total RNA, 0.5 μg, was reverse transcribed into first-strand cDNA using the SuperScript® III First Strand Synthesis System (Invitrogen) according to the manufacturer's protocol. For each sample, a negative control in which the reverse transcriptase enzyme was substituted with distilled water was included to ensure that genomic DNA contamination was not present. Polymerase chain reaction was used to amplify two genes of interest: (1) connexin-43, an important gap junctional protein involved in cell–cell coupling between myocytes, and (2) β-actin, a highly conserved cytoskeletal protein, used here as a housekeeping gene. Sequence-specific primers for these genes, optimized for an annealing temperature of 52°C, were as follows:

Gene	Forward primer (5′–3′)	Reverse primer (5′–3′)
Cx43 (110 bp)	TTCATCATCTTCATGCTGGT	ATCGCTTCTTCCCTTCAC
β-actin (165 bp)	TAAAGACCTCTATGCCAACAC	GATAGAGCCACCAATCCAC

All PCR reactions were done in a reaction volume of 25 μL, and all reagents were obtained from Invitrogen. Two μL of first-strand cDNA was amplified by PCR using the above primers at a final concentration of 0.2 μM along with 0.2 μM dNTPs, 1×PCR Buffer (20 mM Tris-HCl at pH 8.4, 50 mM KCl), 1.5 mM $MgCl_2$, and 0.04 U/μL "Hot start" Platinum® Taq DNA Polymerase. Thermal cycling was performed in a MultiGene II Thermocycler (Labnet International, Woodbridge, NJ) with the following parameters: an initial 2-min denaturation at 94°C, followed by 35 cycles of 94°C for 30 s, 52°C for 30 s, and 72°C for 1 min were performed. A final extension was performed at 72°C for 1 min.

Gel electrophoresis and band densitometry

The PCR products, 6 μL, were loaded in agarose gels (2% w/v in TAE Buffer) with a 100 base pair ladder as a standard. Gel electrophoresis was performed at 100 V for 30 min, and visualization of gels was carried out by ethidium bromide staining under UV light in a BioDoc-It Imaging System (UVP Products, Upland, CA). Band densitometry was performed using the Gel Analyzer option in ImageJ (National Institutes of Health, version 1.36b) to generate lane profile plots. The areas under these curves were measured and expressed as percentages of the total area to produce a semi-quantitative measure of mRNA expression. The resulting intensities for the Cx43 bands and β-actin bands were plotted both as absolute intensities as well as normalized and averaged to give expression of Cx43 relative to β-actin.

Statistical analysis

The nonstimulated and stimulated groups were compared using *T*-test with Sigma Stat 3.0. Normality and equality of variance was tested for all data points. Differences were accepted to be statistically significant at $p < 0.05$.

Results

The Ultrafoam collagen scaffold exhibited an isotropic macroporous structure with large interconnected pores. The average pore diameter was 190 μm, and the average wall thickness was 8 μm, as estimated from the dry-state images (Fig. 1B). Pores as small as 1 μm in diameter and fibers as small as 1.5 μm in diameter were present within the network of large pores. In the hydrated state, macroporous isotropic pore structure was maintained (Fig. 1C).

Optical mapping was used to monitor impulse propagation after point stimulation and to measure the average conduction velocity over the whole mapping area. These studies revealed fast and uniform propagation across the mapping area in the constructs cultivated with electrical field stimulation (Fig. 2A). In contrast, the nonstimulated constructs exhibited nonuniform and slow signal propagation (Fig. 2B). The average conduction velocity recorded for the stimulated constructs (14.4 ± 4.1 cm/s) was significantly higher than that for the nonstimulated constructs (8.6 ± 2.3 cm/s, $p = 0.003$) (Fig. 3A). The maximal conduction velocity measured in the stimulated constructs was 21.4 cm/s, which is similar to the velocity measured in intact neonatal hearts,[30,31] while the smallest measured propagation velocity in the stimulated group was 9.0 cm/s. In the nonstimulated group, we measured 13.0 and 2.6 cm/s as the maximum and minimum value of the propagation velocity, respectively.

Consistent with our previous study, the excitation threshold for electrical field stimulation (the minimum voltage gradient necessary to induce synchronous macroscopic contractions of a tissue construct) was slightly but not significantly lower for stimulated constructs as compared to the nonstimulated constructs (Fig. 3B). The amplitude of construct contraction was evaluated in response to electrical field stimulation at the voltage gradient 50% above the excitation threshold, and calculated as the fractional change in the construct area during the contraction cycle. The amplitude of contractions was significantly higher for the stimulated constructs compared to the constructs cultivated in the absence of electrical field stimulation (Fig. 3C). In response to the electrical field stimulation at 1 Hz, the duration of contraction was comparable for the stimulated and nonstimulated constructs (Fig. 3C), with the average duration of contraction of 533 ± 23 ms for stimulated constructs and 467 ± 83 ms for nonstimulated constructs as measured from the contraction profiles as those depicted in Figure 3C.

Mason's trichrome staining (Fig. 4A, C) was used to determine the presence of cells within the scaffold pores. Because the scaffold is comprised of denatured collagen, it stained red in the trichrome staining (Fig. 4, asterisk). Cell deposited collagen (blue) was present between the cells and on the pore walls (Fig. 4A, C, arrows). Notably, in the stimulated group the cells appeared significantly more elongated, preferentially aligned in parallel to each other and present at higher densities in the scaffold pores. In some regions, the preferential cell alignment appeared to be obstructed by isotropic structure of the scaffold pores (Fig. 4C). In contrast, there was no preferential cell orientation in the nonstimulated group (Fig. 4A), the cell hypertrophy and elongation were not apparent, and the numbers of cells filling the scaffold pores appeared lower than in the stimulated group. Another difference between the two groups was that the nonstimulated constructs contained cells positive for smooth muscle actin at face sections and the surfaces of the construct in direct contact with culture medium (Fig. 4B). In contrast, the staining for smooth muscle actin was completely absent at face sections of stimulated constructs (Fig. 4D), and only occasionally present in the surface layer that was in direct contact with the culture medium (not shown).

Double staining for cardiac troponin I and vimentin revealed the distributions and relative positions of cardiac myocytes and nonmyocytes in the constructs. Consistent with the heterogeneous cell population of the native heart isolate, both nonmyocytes and cardiomyocytes were identified in engineered cardiac constructs (Supplemental Fig. S1A, C,

FIG. 1. Electrical field stimulation cultivation system. (**A**) Set-up for electrical field stimulation consisting of a 100 mm Petri dish fitted with 1/8-inch carbon rods connected to a commercially available cardiac stimulator via platinum wires. (**B**) Cross section of collagen scaffold in dry state. (**C**) Cross section of the collagen scaffold in the hydrate state representing scaffold topography that would be experienced by the cells. Color images available online at www.liebertonline.com/ten.

available online at www.liebertonline.com/ten). In the nonstimulated group, cardiomyocytes (troponin I positive, green, Supplemental Fig. S1A) were randomly dispersed across the construct surface with no preferential orientation. Besides being present on the scaffold surface, the nonmyocytes (vimentin positive, red, Supplemental Fig. S1A) in the nonstimulated group exhibited no preferential directionality and were dispersed among the cardiomyocytes. In the stimulated group, cardiac troponin I–positive cells were found to exhibit preferential alignment (Supplemental Fig. S1C, green), surrounded by nonmyocytes that were located mainly on the construct surfaces (Supplemental Fig. S1C, red). Positive staining for von Willebrand factor was negligible in both groups, indicating the absence of significant number of endothelial cells (Supplemental Fig. S1B, D).

RT-PCR for Cx43 indicated significantly higher expression of this gap junctional protein in the stimulated group than in the nonstimulated group (Fig. 5A). The expression of housekeeping gene, β-actin, was comparable in both groups (Fig. 5). The absence of bands in negative controls, run without the enzyme reverse transcriptase, indicated the absence of genomic contamination and specific amplification of Cx43 transcripts.

Discussion

A hallmark of excitable tissues such as myocardium is the ability to propagate electrical impulses, a property that directly correlates with the tissue functionality. Thus, our goal was to evaluate the velocity of impulse propagation in cardiac tissues cultivated in electrical stimulation bioreactors, using optical mapping. Previously, the velocity of impulse propagation in the ventricles of 2-day-old Sprague Dawley rats was measured to be 25.4 cm/s using a linear electrode array,[30] while the velocity in the heart ventricles of 10-day-old rats was measured to be 27 cm/s.[31] The stimulated constructs in this study exhibited the average propagation velocity of ~55% of that in the native heart, while the highest measured average propagation velocity was ~80% of that measured in the native heart. In contrast, the average propagation velocity in the nonstimulated group was only ~32% of that found in the native heart. The observed impulse propagation velocity was comparable to that reported previously for neonatal rat cardiomyocytes cultivated on the anisotropic poly(glycolic acid) scaffolds.[18] In that previous study, the velocity of impulse propagation in the longitudinal direction (i.e., parallel to the cell and scaffold fibre long axis) was ~15 cm/s at 6 days of cultivation (which is in line with the results reported for our stimulated group cultivated for total of 8 days, Fig. 3A) and increased to ~20 cm/s after 10 days of cultivation. In the transverse direction, the propagation velocity of ~10 cm/s was measured over the entire cultivation period,[18] consistent with the values measured in the present study for the nonstimulated group (Fig. 3B).

The enhanced propagation velocity in the stimulated group was most likely a result of improved cellular elongation and parallel orientation in response to the electrical field gradient, which were observed both in this study (Fig. 4C) and in our previous studies,[25] as well as improved cardiomyocyte coupling suggested by the increase in Cx43

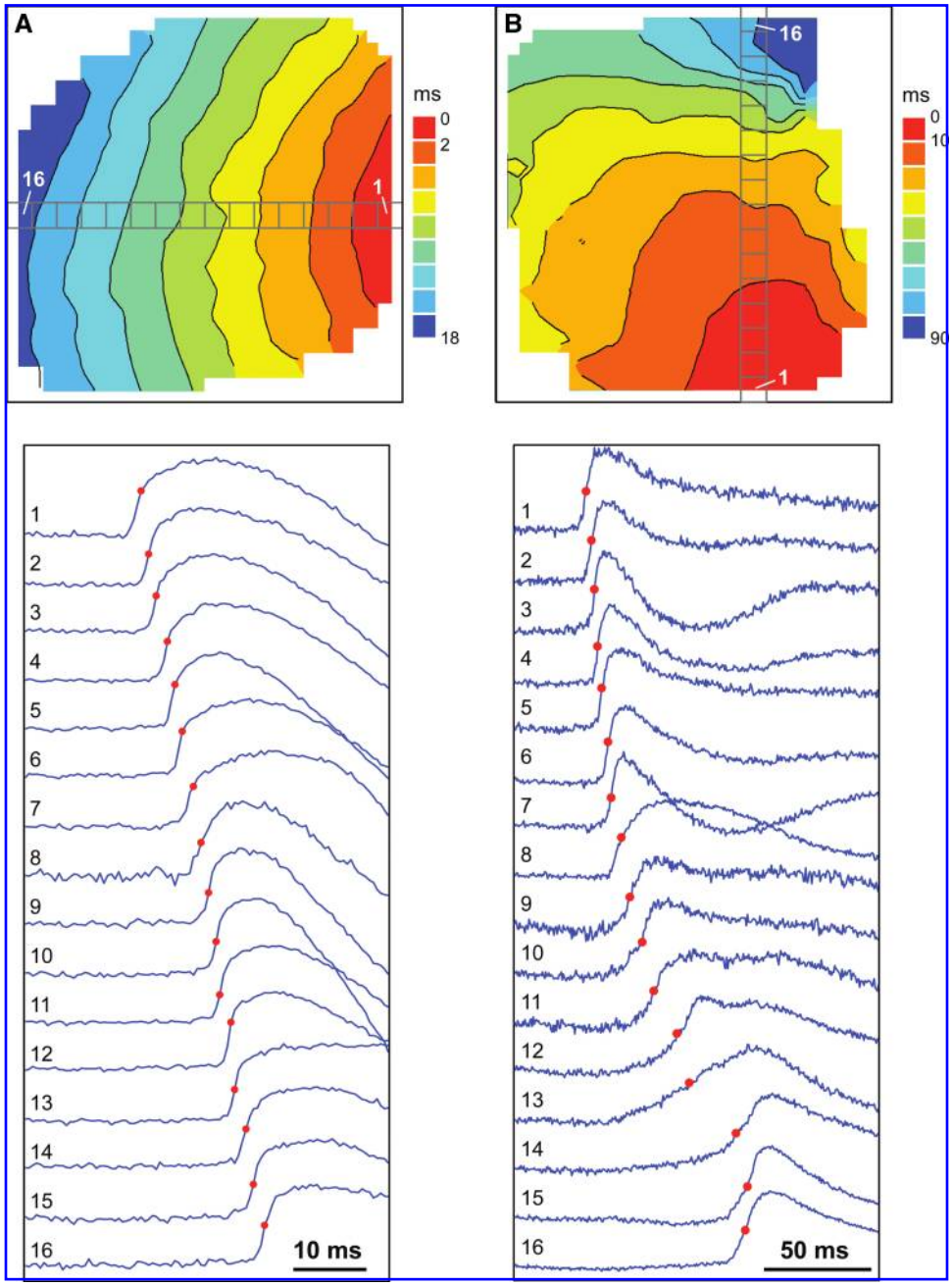

FIG. 2. Optical mapping of activation spread in engineered cardiac tissues. (**A**) Isochronal activation map (top) and selected optical recordings of action potential upstrokes (bottom) in a stimulated tissue sample. (**B**) Activation map and optical recordings in a non-stimulated control. Red circles on optical traces depict activation times. The average conduction velocity was 20.4 and 5.4 cm/s in (**A**) and (**B**), respectively. Color images available online at www.liebertonline.com/ten.

expression (Fig. 5). Cx43 is predominant in the gap junctions of the ventricular cardiomyocytes in the native heart. In our previous studies, using immunostaining for Cx43 and morphometric analysis of TEM images, we demonstrated that the frequency of gap junctions in the stimulated group was comparable to that of the native heart, while in the non-stimulated group the frequency was significantly lower than that of the native heart. It is possible that upon implantation and maturation of the cardiac constructs *in vivo*, the propagation velocity would enhance further. For example, Zimmermann *et al.*[32] reported that cardiac constructs based on neonatal rat cardiomyocytes maintained for 4 weeks in the adult rat myocardium had maximum conduction velocity of 55 ± 16 cm/s longitudinally and 16 ± 7 cm/s transversally, comparable to the conduction velocity in the noninfarcted adult rat myocardium (69 ± 6 cm/s longitudinally and 19 ± 5 cm/s transversally).

Porous collagen scaffold has an isotropic pore structure as illustrated by scanning electron microscopy of the scaffold in dry as well as hydrated state (Fig. 1B, C). The field stimulation and excitation–contraction coupling guide parallel orientation and rearrangement of cardiomyocytes in the stimulated group that is opposed by the isotropic pores that force the elongating cells to "turn-corners" at the pore walls (Fig. 4C). To a certain extent, cells are capable of remodeling the isotropic pore structure via action of cellular proteases and traction forces; however, perfect alignment is hard to achieve with isotropic scaffolds. Several recent studies of cardiomyocyte cultivations on anisotropic scaffolds clearly indicated the importance of scaffold topography in guiding

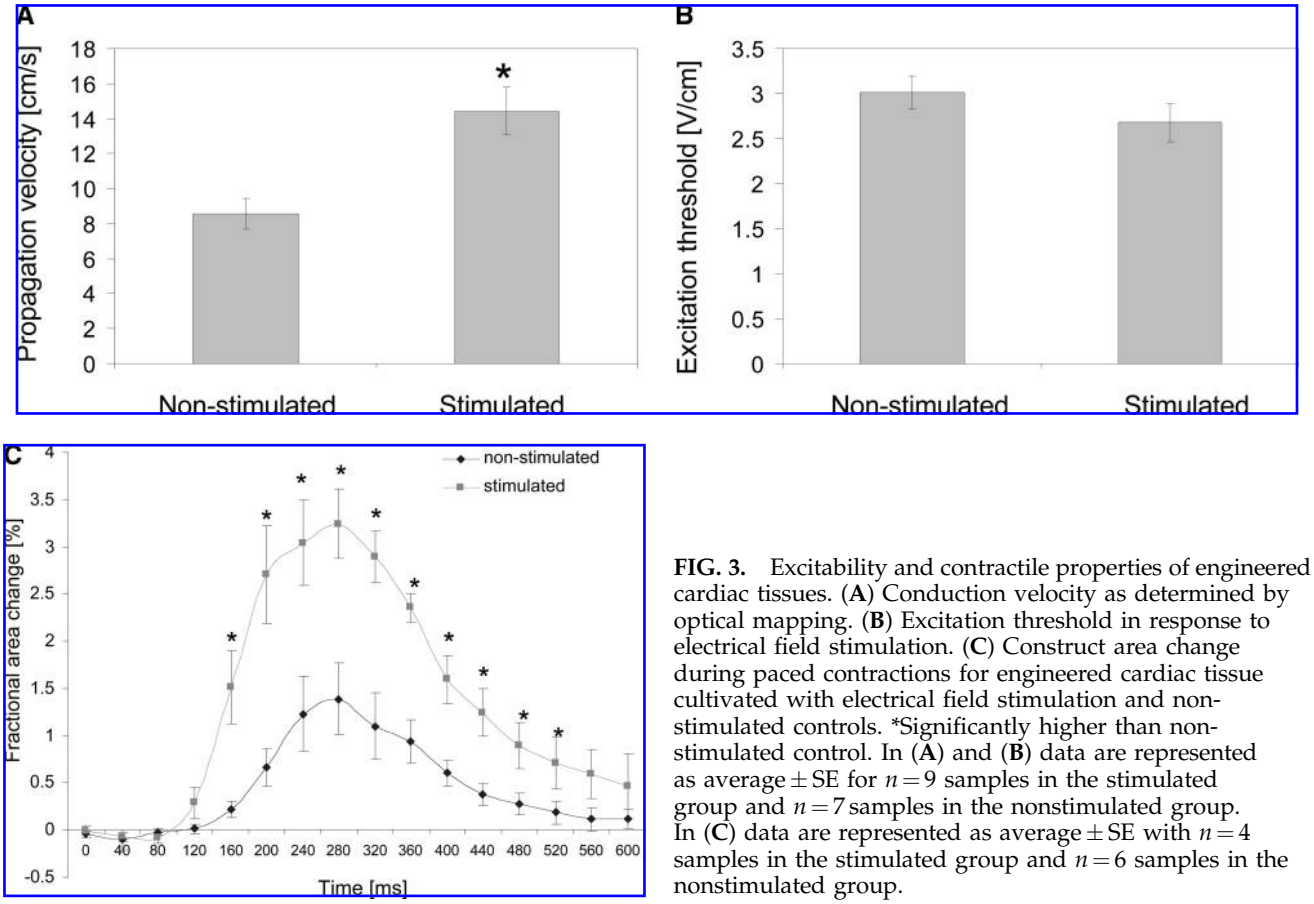

FIG. 3. Excitability and contractile properties of engineered cardiac tissues. (**A**) Conduction velocity as determined by optical mapping. (**B**) Excitation threshold in response to electrical field stimulation. (**C**) Construct area change during paced contractions for engineered cardiac tissue cultivated with electrical field stimulation and non-stimulated controls. *Significantly higher than non-stimulated control. In (**A**) and (**B**) data are represented as average $\pm$ SE for $n = 9$ samples in the stimulated group and $n = 7$ samples in the nonstimulated group. In (**C**) data are represented as average $\pm$ SE with $n = 4$ samples in the stimulated group and $n = 6$ samples in the nonstimulated group.

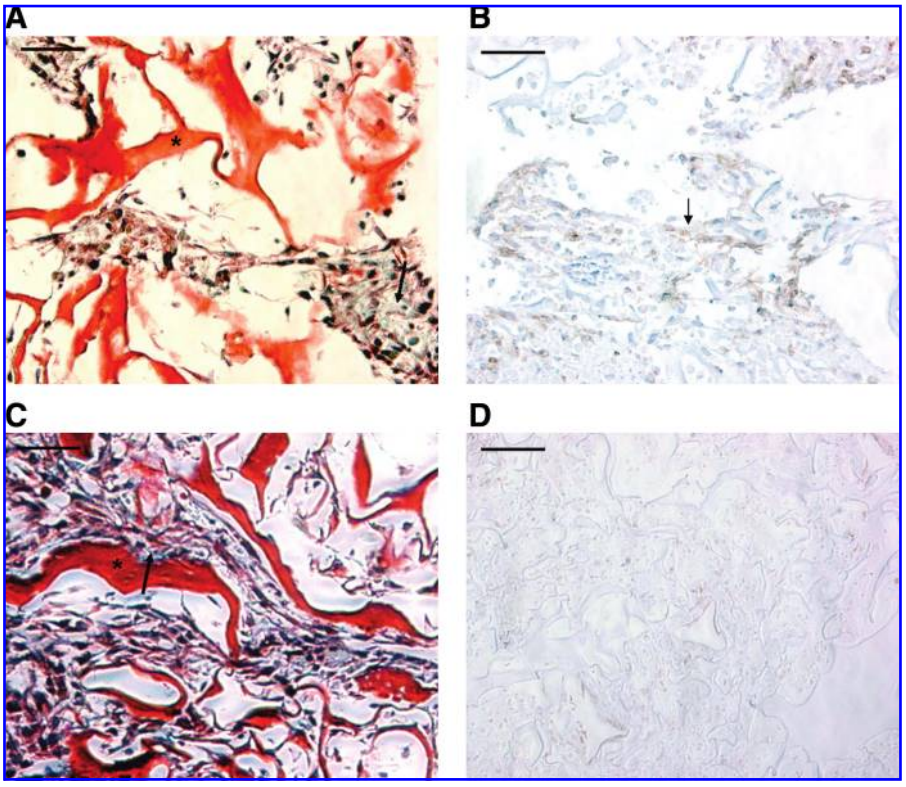

FIG. 4. Histological characterization of engineered cardiac tissue. (**A, B**) Nonstimulated controls. (**C, D**) Stimulated samples. (**A, C**) Mason's trichrome staining. Collagen scaffold stains bright red (*), cells appear dark pink, nuclei appear dark blue, and cell-deposited collagen appears light blue (arrow). (**B, D**) Immunostaining for smooth muscle actin. Positive cells appear brown (arrow). Scale bar: 50 μm. Color images available online at www.liebertonline.com/ten.

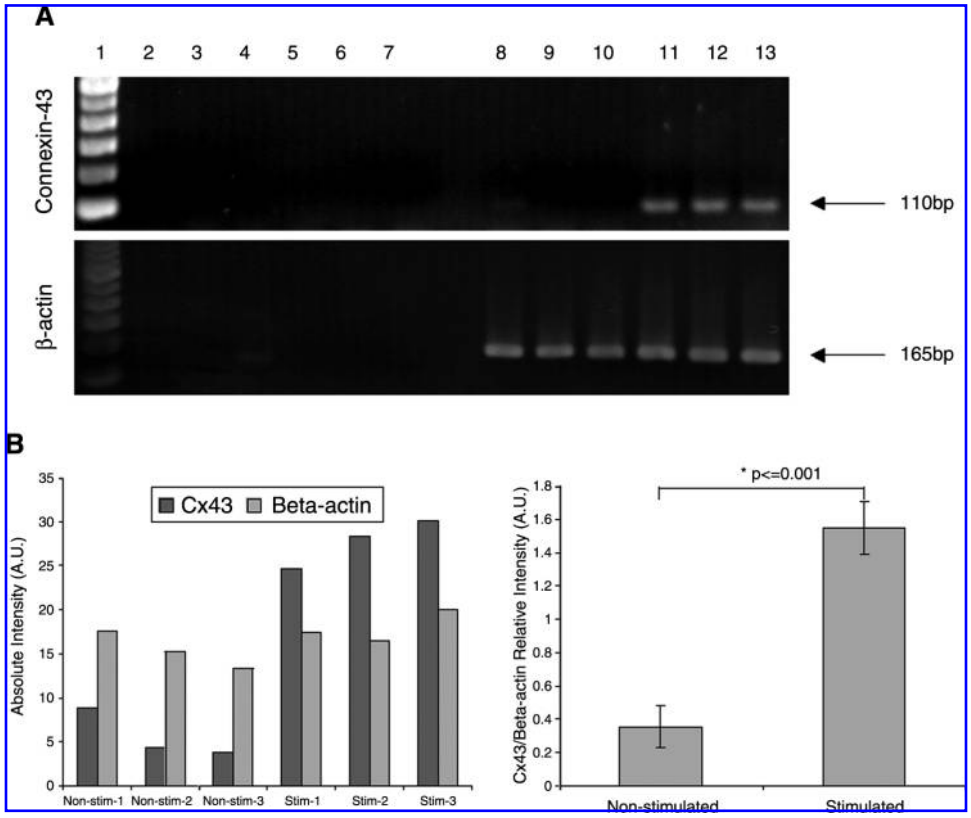

FIG. 5. Expression of gap junctional protein connexin-43. (**A**) Gels showing connexin-43 and β-actin expression. Lane 1, ladder; lanes 2–4, three independent nonstimulated samples subjected to RT-PCR without the reverse transcriptase enzyme; lanes 5–7, three independent stimulated samples subjected to RT-PCR without the reverse transcriptase enzyme; lanes 8–10, three independent nonstimulated samples subjected to RT-PCR with the reverse transcriptase enzyme; lanes 11–13, three independent stimulated samples subjected to RT-PCR with the reverse transcriptase enzyme. (**B**) Densitometric analysis of bands represented in (**A**). (**C**) Relative expression of connexin-43 in comparison to β-actin (connexin-43/β-actin band intensity average ± SD).

functional properties of engineered cardiac structures.[4,18] We expect that cultivation of neonatal rat cardiomyocytes on scaffolds with oriented (anisotropic) pores or fibers in the presence of electrical field stimulation would further enhance the propagation velocity and contractile properties of the engineered cardiac tissue.

Because cardiac fibroblasts can rapidly overgrow cardiomyocytes in monolayer cultures, the cell suspension used for monolayer studies is routinely enriched for cardiomyocytes by preplating. By analogy, early cardiac tissue engineering studies involved the use of cell populations enriched for cardiomyocytes by preplating,[33–37] and some studies demonstrated that the velocity of impulse propagation increased with an increase in the fraction of cardiomyocytes in the cell preparation.[34] Zimmermann, Eschenhagen, and coworkers[23,37] recognized the importance of the presence of multiple cell types for the *in vitro* cultivation of heart tissue in their cultivation system with cyclic stretch. Previously, we characterized only cardiomyocytes in the stimulated and nonstimulated constructs,[25] but in this study we also evaluated the presence of nonmyocytes.

In our hands, the composition of neonatal rat heart cell suspension after one 1 h preplating step was 64 ± 5% cardiomyocytes (cardiac troponin I–positive cells) and 34 ± 16% fibroblasts (prolyl-4-hydroxylase–positive cells),[29] while after two 1 h preplating steps the isolate was enriched for cardiomyocytes (81 ± 14% cardiomyocytes vs. 16 ± 3% fibroblasts). The fraction of other cell types remained low (e.g., 3 ± 3% endothelial cells).[38] During cultivation, the fibroblasts persisted in the constructs but did not overgrow cardiomyocytes (Supplemental Fig. S1), possibly due to the microarchitecture of the scaffold pores.[39] Because endothelial cells were mostly absent in these constructs (Supplemental Fig. S1B, D), coculture or scaffold prevascularization *in vitro* may be required. Alternatively, scaffolds with immobilized angiogenic factors may be utilized[40] to promote rapid vascularization *in vivo*. Interestingly, in the present study there were no smooth muscle actin–positive cells in the face sections of stimulated constructs, while remarkably higher numbers were present in the nonstimulated constructs (Fig. 4). Because smooth muscle cells account for only ~3% of the native heart cell isolate after one preplating,[23] the smooth muscle actin–positive cells in the nonstimulated constructs may be myofibroblasts. The myofibroblasts exhibit elevated secretion of extracellular matrix proteins; they are implicated in scarring upon myocardial infarction[41] and the decrease in propagation velocity when present in critical numbers (e.g., more than 7 myofibroblasts per 100 cardiomyocytes).[42]

Electrical field stimulation bioreactor, such as the one used here, may prove to be a useful tool in engineering cardiac constructs based on human stem/progenitor cell sources. The bioreactor we used is simple to construct and operate, thus enabling easy translation into other research laboratories and ultimately clinical practice. Electrical field stimulation is provided by a pair of parallel carbon electrodes (Fig. 1A), positioned 1 cm apart within a glass chamber and connected to a commercially available stimulator or a custom-made pulse generator/amplifier circuit. In our previous studies we have tested a number of electrode materials (titanium, titanium nitride, and stainless steel) in addition to carbon.[43] We found that carbon was indeed an optimal material for this application due to high resistance to polarization and Faradaic reactions, high efficiency of charge transfer to electrolyte (and hence to the tissue construct), and

low impedance modulus across a large frequency range (10^{-2} to 10^{6} Hz). Further, although the impedance of carbon electrodes decreased with age when low frequencies (e.g., 1 Hz) were used, its resistance to Faradaic reactions remained unchanged, indicating that the same setup can be re-used for numerous experiments. The resistance measured in the bioreactors with carbon rods spaced 1 cm apart was 20Ω and 10Ω for 8- and 4-cm-long electrodes, respectively.[44] Total charge injected with a single 5 V/cm pulse of 2 ms duration in a setup consisting of a 60 mm Petri dish with 20 mL of phosphate buffered saline was measured to be 2.3×10^{-4} C.[43]

The collagen scaffold used in this study was a commercially available hemostat, Ultrafoam, which is water insoluble, and formed from the partial HCl salt of purified bovine dermal (corium) collagen as a sponge with interconnected pores. Because it has already gained FDA approval as a hemostat, this scaffold may indeed be a suitable material for engineering of a clinically relevant cardiac patch. For cell seeding, we used rapid inoculation of the cells at high density with a hydrogel (Matrigel).[2] Because Matrigel is derived from the basement membrane of a mouse sarcoma, it is not suitable for preparation of clinically relevant constructs. Currently, we have complementary efforts underway to replace Matrigel by biodegradable hydrogels of controllable composition based on chitosan[45] or hyaluronic acid.[46]

Approaches to improve the current bioreactor involve development of second-generation bioreactors that incorporate mechanical stimulation[37] or culture medium[17] flow along with electrical field stimulation. One approach to providing mechanical stimulation in such a bioreactor would include pulsatile culture medium flow, where a culture medium pulse would be applied between the electrical pulses. To ensure that the constructs are not moving during an experiment, they can be fixed by pinning into a thin layer of poly(dimethylsiloxane) cast on the bottom of the chamber.[43]

In summary, we demonstrated here that the engineered cardiac tissue cultivated in the presence of electrical field stimulation exhibits impulse propagation comparable to that of the neonatal rat ventricles. The tissues were comprised of multiple cell types, mostly cardiomyocytes and fibroblasts; however, no overgrowth of fibroblasts was observed. In the stimulated group, the fibroblasts were confined to the surface layer of the construct in the direct contact with the culture medium. Endothelial cells were largely absent in both groups, while smooth muscle–positive cells, most likely myofibroblasts, were more numerous in the nonstimulated group than in the stimulated group.

Acknowledgments

This study was supported by NSERC (Discovery Grant to M.R.), NIH (R01 HL076485 and P41-EB002520 to G.V.N.), and Ontario Graduate Scholarship (to R.K.I.).

References

1. Krikpatrick, J.N., Vannan, M.A., Narula, J., and Lang, R.M. Echocardiography in heart failure: applications, utility, and new horizons. J Am Coll Cardiol **50,** 381, 2007.
2. Radisic, M., Euloth, M., Yang, L., Langer, R., Freed, L.E., and Vunjak-Novakovic, G. High-density seeding of myocyte cells for cardiac tissue engineering. Biotechnol Bioeng **82,** 403, 2003.
3. Park, H., Radisic, M., Lim, J.O., Chang, B.H., and Vunjak-Novakovic, G. A novel composite scaffold for cardiac tissue engineering. *In Vitro* Cell Dev Biol Anim **41,** 188, 2005.
4. Zong, X., Bien, H., Chung, C.Y., Yin, L., Fang, D., Hsiao, B.S., Chu, B., and Entcheva, E. Electrospun fine-textured scaffolds for heart tissue constructs. Biomaterials **26,** 5330, 2005.
5. McDevitt, T.C., Woodhouse, K.A., Hauschka, S.D., Murry, C.E., and Stayton, P.S. Spatially organized layers of cardiomyocytes on biodegradable polyurethanefilms for myocardial repair. J Biomed Mater Res A **66,** 586, 2003.
6. Carrier, R.L., Rupnick, M., Langer, R., Schoen, F.J., Freed, L.E., and Vunjak-Novakovic, G. Perfusion improves tissue architecture of engineered cardiac muscle. Tissue Eng **8,** 175, 2002.
7. Boublik, J., Park, H., Radisic, M., Tognana, E., Chen, F., Pei, M., Vunjak-Novakovic, G., and Freed, L.E. Mechanical properties and remodeling of hybrid cardiac constructs made from heart cells, fibrin, and biodegradable, elastomeric knitted fabric. Tissue Eng **11,** 1122, 2005.
8. Badylak, S.F., Kochupura, P.V., Cohen, I.S., Doronin, S.V., Saltman, A.E., Gilbert, T.W., Kelly, D.J., Ignotz, R.A., and Gaudette, G.R. The use of extracellular matrix as an inductive scaffold for the partial replacement of functional myocardium. Cell Transplant **15 Suppl 1,** S29, 2006.
9. Zimmermann, W.H., Didie, M., Doker, S., Melnychenko, I., Naito, H., Rogge, C., Tiburcy, M., and Eschenhagen, T. Heart muscle engineering: an update on cardiac muscle replacement therapy. Cardiovasc Res **71,** 419, 2006.
10. Eschenhagen, T., and Zimmermann, W.H. Engineering myocardial tissue. Circ Res **97,** 1220, 2005.
11. Laflamme, M.A., and Murry, C.E. Regenerating the heart. Nat Biotechnol **23,** 845, 2005.
12. Takahashi, K., and Yamanaka, S. Induction of pluripotent stem cells from mouse embryonic and adult fibroblast cultures by defined factors. Cell **126,** 663, 2006.
13. Takahashi, K., Tanabe, K., Ohnuki, M., Narita, M., Ichisaka, T., Tomoda, K., and Yamanaka, S. Induction of pluripotent stem cells from adult human fibroblasts by defined factors. Cell **131,** 861, 2007.
14. Nakagawa, M., Koyanagi, M., Tanabe, K., Takahashi, K., Ichisaka, T., Aoi, T., Okita, K., Mochiduki, Y., Takizawa, N., and Yamanaka, S. Generation of induced pluripotent stem cells without Myc from mouse and human fibroblasts. Nat Biotechnol **26,** 101, 2008.
15. Park, I.H., Zhao, R., West, J.A., Yabuuchi, A., Huo, H., Ince, T.A., Lerou, P.H., Lensch, M.W., and Daley, G.Q. Reprogramming of human somatic cells to pluripotency with defined factors. Nature **451,** 141, 2008.
16. Lowry, W.E., Richter, L., Yachechko, R., Pyle, A.D., Tchieu, J., Sridharan, R., Clark, A.T., and Plath, K. Generation of human induced pluripotent stem cells from dermal fibroblasts. Proc Natl Acad Sci USA **105,** 2883, 2008.
17. Radisic, M., Yang, L., Boublik, J., Cohen, R.J., Langer, R., Freed, L.E., and Vunjak-Novakovic, G. Medium perfusion enables engineering of compact and contractile cardiac tissue. Am J Physiol Heart Circ Physiol **286,** H507, 2004.
18. Bursac, N., Loo, Y., Leong, K., and Tung, L. Novel anisotropic engineered cardiac tissues: studies of electrical propagation. Biochem Biophys Res Commun **361,** 847, 2007.
19. Nag, A.C. Study of non-muscle cells of the adult mammalian heart: a fine structural analysis and distribution. Cytobios **28,** 41, 1980.
20. Banerjee, I., Yekkala, K., Borg, T.K., and Baudino, T.A. Dynamic interactions between myocytes, fibroblasts, and extracellular matrix. Ann NY Acad Sci **1080,** 76, 2006.

21. Kuzuya, M., and Kinsella, J.L. Induction of endothelial cell differentiation *in vitro* by fibroblast-derived soluble factors. Exp Cell Res **215,** 310, 1994.
22. Seghezzi, G., Patel, S., Ren, C.J., Gualandris, A., Pintucci, G., Robbins, E.S., Shapiro, R.L., Galloway, A.C., Rifkin, D.B., and Mignatti, P. Fibroblast growth factor-2 (FGF-2) induces vascular endothelial growth factor (VEGF) expression in the endothelial cells of forming capillaries: an autocrine mechanism contributing to angiogenesis. J Cell Biol **141,** 1659, 1998.
23. Naito, H., Melnychenko, I., Didie, M., Schneiderbanger, K., Schubert, P., Rosenkranz, S., Eschenhagen, T., and Zimmermann, W.H. Optimizing engineered heart tissue for therapeutic applications as surrogate heart muscle. Circulation **114,** I72, 2006.
24. Radisic, M., Park, H., Martens, T.P., Salazar-Lazaro, J.E., Geng, W., Wang, Y., Langer, R., Freed, L.E., and Vunjak-Novakovic, G. Pre-treatment of synthetic elastomeric scaffolds by cardiac fibroblasts improves engineered heart tissue. J Biomed Mater Res A 2007.
25. Radisic, M., Park, H., Shing, H., Consi, T., Schoen, F.J., Langer, R., Freed, L.E., and Vunjak-Novakovic, G. Functional assembly of engineered myocardium by electrical stimulation of cardiac myocytes cultured on scaffolds. Proc Natl Acad Sci USA **101,** 18129, 2004.
26. Fast, V.G., and Cheek, E.R. Optical mapping of arrhythmias induced by strong electrical shocks in myocyte cultures. Circ Res **90,** 664, 2002.
27. Fast, V.G. Recording action potentials using voltage-sensitive dyes. In: Dhein, S., Delmar, M., and Mohr, F.W., eds. Methods in Cardiovascular Research. Berlin: Springer-Verlag, 2005, p. 233–255.
28. Radisic, M., Park, H., Chen, F., Salazar-Lazzaro, J.E., Wang, Y., Dennis, R., Langer, R., Freed, L.E., and Vunjak-Novakovic, G. Biomimetic approach to cardiac tissue engineering: oxygen carriers and channeled scaffolds. Tissue Eng **12,** 2077, 2006.
29. Radisic, M., Marsano, A., Maidhof, R., Wang, Y., and Vunjak-Novakovic, G. Cardiac tissue engineering using perfusion bioreactor systems. Nature Protocols **3,** 719, 2008.
30. Bursac, N., Papadaki, M., Langer, R., Eisenberg, S.R., Vunjak-Novakovic, G., and Freed, L.E. Towards a functional tissue engineered cardiac muscle. 21st Annual Meeting of the Biomedical Engineering Society, Atlanta, 1999, p. 29.
31. Sun, L.S., Legato, M.J., Rosen, T.S., Steinberg, S.F., and Rosen, M.R. Sympathetic innervation modulates ventricular impulse propagation and repolarisation in the immature rat heart. Cardiovasc Res **27,** 459, 1993.
32. Zimmermann, W.H., Melnychenko, I., Wasmeier, G., Didie, M., Naito, H., Nixdorff, U., Hess, A., Budinsky, L., Brune, K., Michaelis, B., Dhein, S., Schwoerer, A., Ehmke, H., and Eschenhagen, T. Engineered heart tissue grafts improve systolic and diastolic function in infarcted rat hearts. Nat Med **12,** 452, 2006.
33. Carrier, R.L., Papadaki, M., Rupnick, M., Schoen, F.J., Bursac, N., Langer, R., Freed, L.E., and Vunjak-Novakovic, G. Cardiac tissue engineering: cell seeding, cultivation parameters and tissue construct characterization. Biotechnol Bioeng **64,** 580, 1999.
34. Bursac, N., Papadaki, M., Cohen, R.J., Schoen, F.J., Eisenberg, S.R., Carrier, R., Vunjak-Novakovic, G., and Freed, L.E. Cardiac muscle tissue engineering: toward an *in vitro* model for electrophysiological studies. Am J Physiol Heart Circ Physiol **277,** H433, 1999.
35. Fink, C., Ergun, S., Kralisch, D., Remmers, U., Weil, J., and Eschenhagen, T. Chronic stretch of engineered heart tissue induces hypertrophy and functional improvement. FASEB J **14,** 669, 2000.
36. Papadaki, M., Bursac, N., Langer, R., Merok, J., Vunjak-Novakovic, G., and Freed, L.E. Tissue engineering of functional cardiac muscle: molecular, structural and electrophysiological studies. Am J Physiol Heart Circ Physiol **280,** H168, 2001.
37. Zimmermann, W.H., Schneiderbanger, K., Schubert, P., Didie, M., Munzel, F., Heubach, J.F., Kostin, S., Nehuber, W.L., and Eschenhagen, T. Tissue engineering of a differentiated cardiac muscle construct. Circ Res **90,** 223, 2002.
38. Iyer, R., Chiu, L., and Radisic, M. Microfabricated poly(ethylene glycol) templates enable rapid screening of triculture conditions for cardiac tissue engineering. J Biomed Mater Res Part A, 2008. [Epub ahead of print]
39. Boateng, S.Y., Hartman, T.J., Ahluwalia, N., Vidula, H., Desai, T.A., and Russell, B. Inhibition of fibroblast proliferation in cardiac myocyte cultures by surface microtopography. Am J Physiol Cell Physiol **285,** C171, 2003.
40. Shen, Y.H., Shoichet, M.S., and Radisic, M. Vascular endothelial growth factor immobilized in collagen scaffold promotes penetration and proliferation of endothelial cells. Acta Biomater **4,** 477, 2008.
41. Sun, Y., Kiani, M.F., Postlethwaite, A.E., and Weber, K.T. Infarct scar as living tissue. Basic Res Cardiol **97,** 343, 2002.
42. Miragoli, M., Gaudesius, G., and Rohr, S. Electrotonic modulation of cardiac impulse conduction by myofibroblasts. Circ Res **98,** 801, 2006.
43. Cannizzaro, C., Tandon, N., Figallo, E., Park, H., Gerecht, S., Radisic, M., Elvassore, N., and Vunjak-Novakovic, G. Practical aspects of cardiac tissue engineering with electrical stimulation. Methods Mol Med **140,** 291, 2007.
44. Tandon, N., Cannizzaro, C., Chao, G., Maidhof, R., Marsano, A., Au, H., Radisic, M., and Vunjak-Novakovic, G. Electrical stimulation systems for cardiac tissue engineering. Nat Protoc [in press].
45. Yeo, Y., Geng, W., Ito, T., Kohane, D.S., Burdick, J.A., and Radisic, M. Photocrosslinkable hydrogel for myocyte cell culture and injection. J Biomed Mater Res B Appl Biomater **81,** 312, 2007.
46. Gerecht, S., Burdick, J.A., Ferreira, L.S., Townsend, S.A., Langer, R., and Vunjak-Novakovic, G. Hyaluronic acid hydrogel for controlled self-renewal and differentiation of human embryonic stem cells. Proc Natl Acad Sci USA **104,** 11298, 2007.

Address reprint requests to:
Milica Radisic, Ph.D.
Institute of Biomaterials and Biomedical Engineering
University of Toronto
164 College St., Room 407
Toronto, Ontario M5S 3G9
Canada

E-mail: m.radisic@utoronto.ca

Gordana Vunjak-Novakovic, Ph.D.
Department of Biomedical Engineering
Columbia University Vanderbilt Clinic
12th Floor, Room 12-234 622, West 168th St.
New York, NY 10032

E-mail: gv2131@columbia.edu

Received: April 16, 2008
Accepted: July 28, 2008
Online Publication Date: October 6, 2008

This article has been cited by:

1. Maximilian Y. Emmert, Robert W. Hitchcock, Simon P. Hoerstrup. 2013. Cell therapy, 3D culture systems and tissue engineering for cardiac regeneration. *Advanced Drug Delivery Reviews* . [CrossRef]
2. Zlata Vukadinovic-Nikolic, Birgit Andrée, Suzanne E. Dorfman, Michael Pflaum, Tibor Horvath, Marco Lux, Letizia Venturini, Antonia Bär, George Kensah, Angelica Roa Lara, Igor Tudorache, Serghei Cebotari, Denise Hilfiker-Kleiner, Axel Haverich, Andres Hilfiker. Generation of Bioartificial Heart Tissue by Combining a Three-Dimensional Gel-Based Cardiac Construct with Decellularized Small Intestinal Submucosa. *Tissue Engineering Part A*, ahead of print. [Abstract] [Full Text HTML] [Full Text PDF] [Full Text PDF with Links] [Supplemental Material]
3. Dr. Zlata Vukadinovic-Nikolic, Dr. Birgit Andrée, Dr. Suzanne E. Dorfman, Michael Pflaum, Tibor Horvath, Marco Lux, Letizia Venturini, Dr. Antonia Bär, Mr. George Kensah, Dr. Angelica Roa Lara, Dr. Igor Tudorache, Dr. Serghei Cebotari, Prof. Denise Hilfiker-Kleiner, Dr. Axel Haverich, Dr. Andres Hilfiker. Generation of bioartificial heart tissue by combining a 3D gel-based cardiac construct with decellularized small intestinal submucosa. *Tissue Engineering Part A* **0**:ja. . [Abstract] [Full Text PDF] [Full Text PDF with Links]
4. Vishal Tandon, Boyang Zhang, Milica Radisic, Shashi K. Murthy. 2013. Generation of tissue constructs for cardiovascular regenerative medicine: From cell procurement to scaffold design. *Biotechnology Advances* **31**:5, 722-735. [CrossRef]
5. Giancarlo Forte, Stefania Pagliari, Francesca Pagliari, Mitsuhiro Ebara, Paolo Nardo, Takao Aoyagi. 2013. Towards the Generation of Patient-Specific Patches for Cardiac Repair. *Stem Cell Reviews and Reports* **9**:3, 313-325. [CrossRef]
6. Loraine LY Chiu, Milica Radisic. 2013. Cardiac tissue engineering. *Current Opinion in Chemical Engineering* **2**:1, 41-52. [CrossRef]
7. J Roether, H Jawad, R Rai, N Ali, S Harding, A BoccaciniPolymers for Myocardial Tissue Engineering 369-388. [CrossRef]
8. Nimalan Thavandiran, Sara S Nunes, Yun Xiao, Milica Radisic. 2013. Topological and electrical control of cardiac differentiation and assembly. *Stem Cell Research & Therapy* **4**:1, 14. [CrossRef]
9. Deborah K. Lieu, Irene C. Turnbull, Kevin D. Costa, Ronald A. Li. 2012. Engineered human pluripotent stem cell-derived cardiac cells and tissues for electrophysiological studies. *Drug Discovery Today: Disease Models* **9**:4, e209-e217. [CrossRef]
10. Claus Svane Sondergaard, Grant Mathews, Lianguo Wang, Angela Jeffreys, Amrit Sahota, Moira Wood, Crystal M. Ripplinger, Ming-Sing Si. 2012. Contractile and Electrophysiologic Characterization of Optimized Self-Organizing Engineered Heart Tissue. *The Annals of Thoracic Surgery* **94**:4, 1241-1249. [CrossRef]
11. Brian Liau, Donghui Zhang, Nenad Bursac. 2012. Functional cardiac tissue engineering. *Regenerative Medicine* **7**:2, 187-206. [CrossRef]
12. Jennifer Dawson, Olivier Schussler, Ashraf Al-Madhoun, Claudine Menard, Marc Ruel, Ilona S. Skerjanc. 2011. Collagen scaffolds with or without the addition of RGD peptides support cardiomyogenesis after aggregation of mouse embryonic stem cells. *In Vitro Cellular & Developmental Biology - Animal* . [CrossRef]
13. Stephen F. Badylak, Doris Taylor, Korkut Uygun. 2011. Whole-Organ Tissue Engineering: Decellularization and Recellularization of Three-Dimensional Matrix Scaffolds. *Annual Review of Biomedical Engineering* **13**:1, 27-53. [CrossRef]
14. Jana Dengler, Hannah Song, Nimalan Thavandiran, Stéphane Massé, Geoffrey A. Wood, Kumaraswamy Nanthakumar, Peter W. Zandstra, Milica Radisic. 2011. Engineered heart tissue enables study of residual undifferentiated embryonic stem cell activity in a cardiac environment. *Biotechnology and Bioengineering* **108**:3, 704-719. [CrossRef]
15. P. Akhyari, M. Barth, A. LichtenbergCardiac Patch with Cells: Biological or Synthetic 367-388. [CrossRef]
16. Loraine L. Y. Chiu, Milica Radisic, Gordana Vunjak-Novakovic. 2010. Bioactive Scaffolds for Engineering Vascularized Cardiac Tissues. *Macromolecular Bioscience* **10**:11, 1286-1301. [CrossRef]
17. Peter C. Johnson, Antonios G. MikosStem Cells: State of the Art 3-11. [Citation] [Full Text PDF] [Full Text PDF with Links]
18. C. Katherine Chiang, Mohammad Fahad Chowdhury, Rohin K. Iyer, William L. Stanford, Milica Radisic. 2010. Engineering surfaces for site-specific vascular differentiation of mouse embryonic stem cells. *Acta Biomaterialia* **6**:6, 1904-1916. [CrossRef]
19. Marta Codina, Jeremy Elser, Kenneth B. Margulies. 2010. Current Status of Stem Cell Therapy in Heart Failure. *Current Cardiology Reports* **12**:3, 199-208. [CrossRef]
20. Gordana Vunjak-Novakovic, Nina Tandon, Amandine Godier, Robert Maidhof, Anna Marsano, Timothy P. Martens, Milica Radisic. 2010. Challenges in Cardiac Tissue Engineering. *Tissue Engineering Part B: Reviews* **16**:2, 169-187. [Abstract] [Full Text HTML] [Full Text PDF] [Full Text PDF with Links]
21. Loraine L.Y. Chiu, Milica Radisic. 2010. Scaffolds with covalently immobilized VEGF and Angiopoietin-1 for vascularization of engineered tissues. *Biomaterials* **31**:2, 226-241. [CrossRef]

22. Peter C. Johnson, Antonios G. MikosAdvances in Tissue Engineering: Volume 2 . [Citation] [Full Text HTML] [Full Text PDF] [Full Text PDF with Links]